Design and Development of Damping Sandwich Panels for Satellite Housing Using Additive Manufacturing

Matija Milenovic[1,a], Huina Mao[1,b[0000−0001−9980−0144]], Bernd Peukert[2,c[0000−0001−9499−172X]], Gunnar Tibert[1,d[0000−0001−6802−8331]], and Sasan Dadbakhsh[2,e[0000−0003−4120−4790]]

[1] Department of Engineering Mechanics, KTH Royal Institute of Technology, SE-10044, Stockholm, Sweden
[2] Production Engineering Department, KTH Royal Institute of Technology, SE-10044, Stockholm,
[a]matija@porkchop.space, [b]huina@kth.se, [c]bpeuke@kth.se
[d]tibert@kth.se, [e]sdad@kth.se

Abstract. The present work investigates the performance of additively-manufactured sandwich structures with the goal of reducing the effect of vibrations on a spacecraft during launch, whilst minimizing mass. Additive manufacturing allows designers to implement custom and complex geometries, such as the sheet gyroid structures, inside sandwich panels. Accordingly, this work details the development of gyroid-based sandwich structures for damping. Several test specimens are designed, additively manufactured using ABS plastic, and their damping performances are evaluated based on both simulation and experiments. Damping values are identified using frequency response transfer functions. The results show that as theory predicts, adding more mass, through the added thickness of the gyroid reduces the amplitude of vibrations. However, on a damping-per-unit-mass basis, the experimental results are inconclusive mainly due to the measurements of vibrations in the center of the sandwich panels instead of the sides where the vibrations can be maximum. Therefore, simulations better illustrate the changes of the damping behavior at different applied frequencies. Lessons and experiences are summarized for future work, particularly in exploring the effects of varying other 3D printed composite meta-lattice sandwich structures for satellites.

Keywords: Additive Manufacturing · Damping · Sandwich panels · Gyroid · Meta-lattice sandwich.

1 Introduction

Spacecraft experience significant vibration during launch, creating possible problems for the spacecraft even before reaching orbit. Achieving superior vibration suppression to hold the subsystems in place, yet with high load-bearing capabilities during testing, launch, and mission operations in lightweight structural

designs is still a challenge. Sandwich structures are a subset of the composite materials family, consisting of two thin face-sheets and an intermediate core to provide high stiffness/strength and ultra-light structural weight characteristics. They have been extensively utilized in aerospace, automobiles and civil engineering. The Voyager spacecraft, launched in 1977, had antenna reflectors that were made of an aluminum honeycomb core sandwich structure [1]. More recently, the Juno and Cassini spacecraft which travelled to Jupiter and Saturn, respectively, both made use of either composite and/or sandwich structures in order to reduce mass [2]. Today's sandwich structures used in the space industry are primarily made from aluminium alloys (both faces and core) as well as Carbon Fibre-Reinforced Polymer (CFRP). This is since both materials offer high strength per unit mass. Compared with the most common sandwich structures with traditional foam or honeycomb cores for spacecraft and launch vehicles, the newly developed meta-lattice sandwich structures have been providing great potential for multi-functional applications in both mechanics and acoustics[3,4].

Additive manufacturing (AM), also known as 3D printing, has been increasingly used in recent years since it can provide many advantages to the future of space flight, e.g., producing metal and ceramic flight parts, using AM to build entire rockets and their engines [5]. The technology has also been investigated for use in the manufacture of sandwich structures [6]. This has the added advantage that the manufacturing time and cost of sandwich structures could be potentially reduced since only a single machine and material are being used.

The purpose of this research is to explore novel 3D printed structures to reduce the effect of vibrations, particularly during the launch of a spacecraft. The goal of this thesis is to develop a complex sandwich structure with the aim of improving the damping of vibrations when used as part of the spacecraft's structure. This will be achieved by free-form design, 3D printing, and experimental evaluation of the structures. Simulations will be performed to support the analysis of the experimental results. The potential benefits of this technology are certainly not limited to spacecraft. In the context of space exploration, this technology could be used in lunar/martian rovers to aid the suspension when traversing bumpy terrain. Terrestrial benefactors would include the aeronautical, automotive, rail, and naval industries, which each experience similar load cases. The vibration damping properties of strut-based lattice structures consist of struts and nodes that have been extensively studied [7,8,9], and were therefore not part of the scope of this work. Unlike strut-based lattice structures, triply-periodic minimal surface structures are less limited by maximum inclination angle during the AM process since their angle is continuously changing, allowing for better support itself. The Schoen gyroid structure, discovered by Alan Schoen in 1970 [10], is a type of triply-periodic minimal surface structure found in nature, e.g., butterfly wings, mitachondria, and copolymer structures. More importantly, gyroids have shown exceptional mechanical properties in bending, energy absorption, and thermal properties [11,12]. Furthermore, to the best of the author's knowledge, the damping properties of gyroids printed using Acrylonitrile butadiene styrene (ABS) have not yet been extensively documented,

and this paper will therefore serve to benefit future works in this area by being a starting reference point.

2 Methods

2.1 Gyroid sandwich structure specimen

The Schoen gyroid, discovered in 1970 [10], was using rather complex elliptical equations. Here, an implicit trigonometric equation was used to approximate the gyroid geometry as

$$\sin\left(\frac{2\pi}{a}x\right)\cos\left(\frac{2\pi}{a}y\right)+\sin\left(\frac{2\pi}{a}y\right)\cos\left(\frac{2\pi}{a}z\right)+\sin\left(\frac{2\pi}{a}z\right)\cos\left(\frac{2\pi}{a}x\right)=t \tag{1}$$

where x, y, z are spatial parameters, t is the iso-value, and a is periodicity. When $t = 0$, the gyroid is known as a sheet gyroid, whereas for $t \neq 0$, it is known as a cell gyroid (sometimes known as strut gyroid). The number of unit cells was kept constant for this work with $3 \times 3 \times 1$ unit cells of $a = 30$ mm, and instead, the effect of varying gyroid thickness was investigated.

The volume fraction (VF) or solid volume fraction of a lattice structure is defined as the ratio of the actual volume of the lattice itself to the volume of the cuboidal envelope it occupies. In the case of a gyroid, the volume fraction can be computed as

$$VF = \frac{t_G S}{xyz} \tag{2}$$

where t_G is the thickness of the gyroid unit cell, S is the surface area of the gyroid inside the xyz-domain. Three different specimens were designed - with 18%, 31%, and 62% VF.

Stratasys® ABS M30 was chosen as the material for this work as it is a readily-available FDM material, and is easy to work with reducing the possibility of issues during manufacturing (density 1.07 g/cm^3, Young's Modulus 2000 MPa, flexural Modulus 2300 MPa, Max strain 4%, impact toughness $\sim$ 3J/cm). Polycarbonate (PC) was also considered as it is also compatible with the available printer, however, since its material properties are similar to ABS, and are somewhat more difficult to print, it was not used in this study.

All of the gyroid-based sandwich structure specimens used in this work were printed using the Stratasys® Fortus 400 MC FDM printer, as shown in Fig. 1. In order to try to improve the damping of the specimens, another specimen design was proposed: a gyroid specimen with closed walls, and openings on the top for a fluid to be poured in, named as closed-wall specimens, as shown in Fig. 1b. The hypothesis was that adding some amount of fluid inside the gyroid structure would further reduce the amplitude of its vibrations. The fluid chosen for this study was a form of hydraulic oil, commonly used in machinery, and readily available. The oil used was Shell Tellus Oil S 68 (density 0.89 g/cm^3 at 15°C, kinematic viscosity 0.00022 m^2/s at 20°C). The primary reason for selecting this as the filling fluid, apart from its wide availability in the industry, was its low

density. The closed-wall specimens were built with the same volume fractions as their open-wall counterparts (18%, 31%, and 62% VF), using the same material and printer. In order to be able to pour the oil in, two feed holes were placed at the top of the specimen (one for pouring, and the other for air to escape through). The hole diameter was chosen when doing a trade-off between not being too large so as to excessively interfere with the specimen walls, but also not being too small such that it is too difficult to pour the oil inside; therefore, a diameter of 2 mm was chosen.

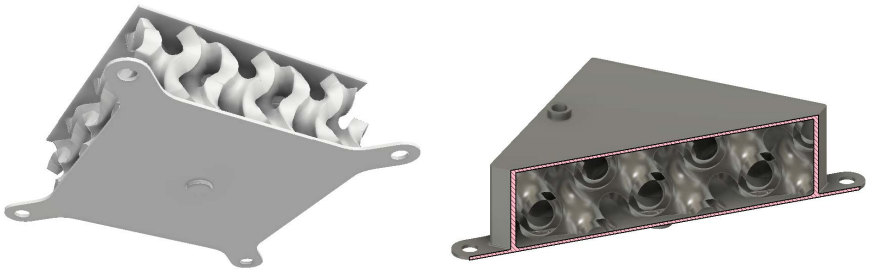

(a) (b)

Fig. 1: a) open gyroid specimen, b) closed-wall gyroid specimen. The gyroid specimen was modified to accommodate the experimental equipment. The side holes are for interfacing with the steel plate, while the bottom cylinder is for interfacing with the shaker.

2.2 Experimental setup

Fig. 2 shows the experimental setup. The force sensor and accelerometer used in the experiment were the Dytran 1053 and 3023, respectively. The vibration shaker was a TIRA TV 50018, and a TTi TG215 was used as the signal generator. The input excitation frequency was controlled using a chirp signal (also known as a frequency sweep signal), ranging from 0–10 kHz. The sampling frequency for all experiments was 20.48 kHz, fulfilling the Nyquist sampling frequency criterion up to 10 kHz. Each run lasted up to 240 s, ensuring that each frequency's response could be properly captured. Five runs were performed for each of the open-wall specimens, while three runs were performed for each filling factor in the closed-wall specimens, of which there were four (thus 12 runs in total for each of the closed-wall specimens). An identical number of runs were performed using another signal generator, however, this generator did not produce a sufficiently large amplitude input signal to the shaker and therefore reduced the signal-to-noise ratio.

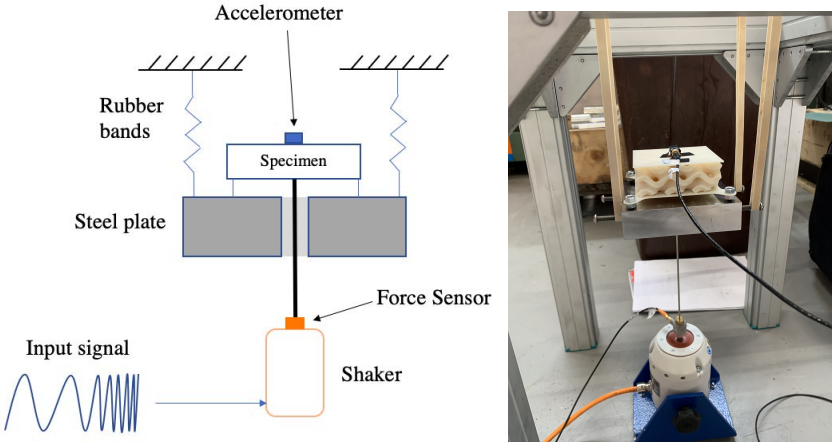

(a) (b)

Fig. 2: Experimental setup: a) schematic, b) experiment.

2.3 Simulation Method

Simulations were performed in order to compare the results of the experiments with finite element method software. After evaluating several possible tools and workflows, ultimately a combination of MathMod, Blender®, and Autodesk Fusion 360™ were best suited for the simulation part of this thesis, as the workflow shown in Fig. 3. The simulations were modal analyses of some of the specimens (specifically the control specimens, and both the open and closed, 18% VF specimens), whereby the mode shapes and frequencies were computed. A standard boundary condition was applied to all specimens: at the flaps, the same way as the specimens in the experiments.

3 Results and discussion

3.1 Experiment results

Table 1 shows that the actual masses of the 3D-printed gyroid specimens have an acceptable coherence with the predicted theoretical masses (with a deviation $< 4.1\%$ for open-wall and $< 6.4\%$ for closed-wall specimens). Here, the isovolumetric and isomassive are for reference comparison, demonstrating blocks with the volume and mass of the sandwich panels, respectively. Accordingly, the Isovolumetric specimen is the heaviest. The 18% VF open- and closed-wall specimens have close masses to the isomassive one, which is only nearly half the mass of the Isovolumetric specimen. As expected, the masses of the open- and closed-wall specimens increased as the VF increased, and the close-wall specimens are heavier than the open-wall specimens of the same VF.

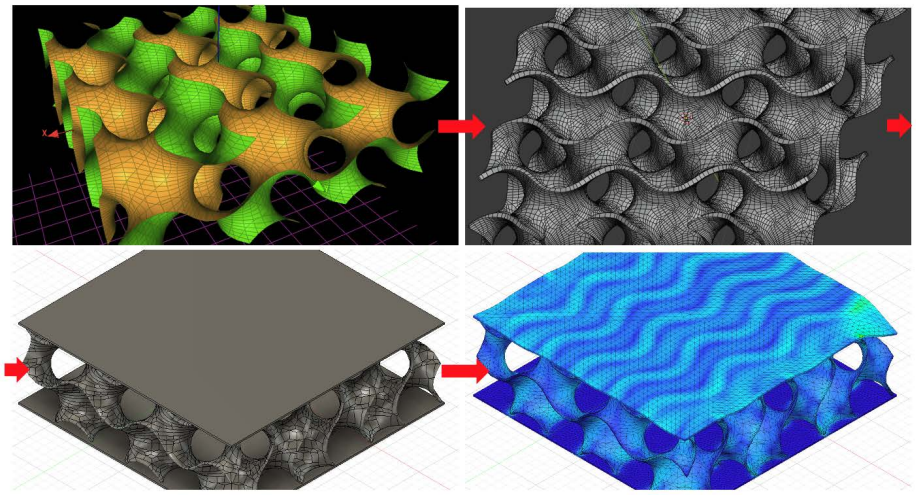

Fig. 3: Process workflow. Clockwise from top-left: Tetrahedral mesh generation in MathMod. Smoothed closed mesh generation in Blender.

Table 1: Theoretical and actual masses of the specimens.

	REF 1	REF 2	Open-wall (VF)			Closed-wall (VF)		
	Isomassive	Isovolumetric	18%	31%	62%	18%	31%	62%
Theoretical Mass (g)	104	259	67	102	146	94	113	171
Actual Mass (g)	97	238	65	98	140	88	106	166
Error (%)	6.7	8.1	3.0	3.9	4.1	6.4	6.2	2.9

Fig. 4 and Fig. 5 show the amplitude of the acceleration per unit force of open-wall specimens and empty closed-wall specimens respectively. The isomassive specimen has the lowest amplitude under the vibration although that is much lighter than the isovolumetric one (Table.1). This indicates the isomassive specimen has better damping properties. No strong pattern can be seen in comparing the open-wall specimens for various VF, Fig. 4, which shows that the shapes of the geometry mostly determine the damping properties, and the thickness of the gyroids studied here is not as critical as expected although an increased mass for a higher VF specimen. This is also found in the closed-wall specimens, Fig. 5, but as the VF increased the added mass is clearly distinguishable at the first modal peak, where the heavier specimens (or higher VF) have lower amplitudes and lower first-mode frequencies.

A comparison of the various open-wall specimens versus the closed-wall specimens is presented in Fig. 7. The largest difference between open- and closed-wall specimens is visible at the low-frequency part of the spectrum (< 500 Hz). The amplitude of the closed-wall peaks is lower, and their first modes are shifted to the right, primarily due to the added stiffness. Both open- and closed-wall

specimens show a relatively lower amplitude acceleration under the vibration in a high-frequency range (> 1000 Hz).

Fig. 8 shows the specific damping (the damping divided and normalised by the weight of each specimen) of each specimen at the first modal peak, which indicates that at a larger VF, the added mass of oil makes a less significant difference in increasing damping. There may also be a "break-even point" wherein a larger VF worsens specific damping.

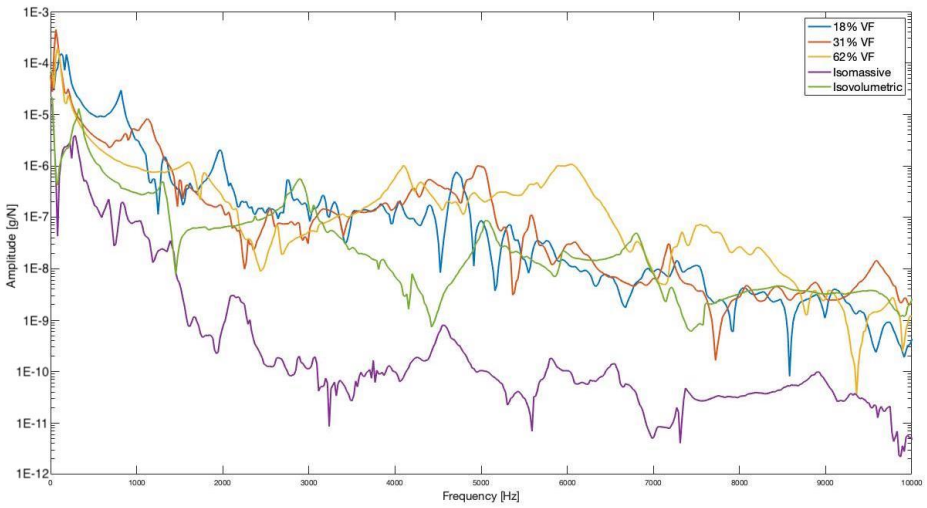

Fig. 4: Acceleration per unit force of various open-wall specimens alongside control specimens.

3.2 Simulation Results

In order to better understand the dynamic properties of the design, modal analysis was performed and compared with experiments, as shown in Table 2. There was very little correlation between the modal frequencies predicted by the simulations and those observed experimentally, as shown in Table 2. Since this was observed across the board, even for the simple-geometry control specimens, it implies that there is likely a flaw in the simulation method. The theoretical mass of each specimen (computed using its geometric volume multiplied by the density of ABS) was consistently greater than the actual measured mass, meaning that the porosity of the printed parts likely introduced a source of error. A distinction was not made between rigid-body and elastic vibration modes neither in simulations nor in experiments, therefore, this may be another possible explanation for discrepancies between the two. In addition, the specimens used in this work were limited to $90 \times 90 \times 30$ mm^3, which represents an "element" of

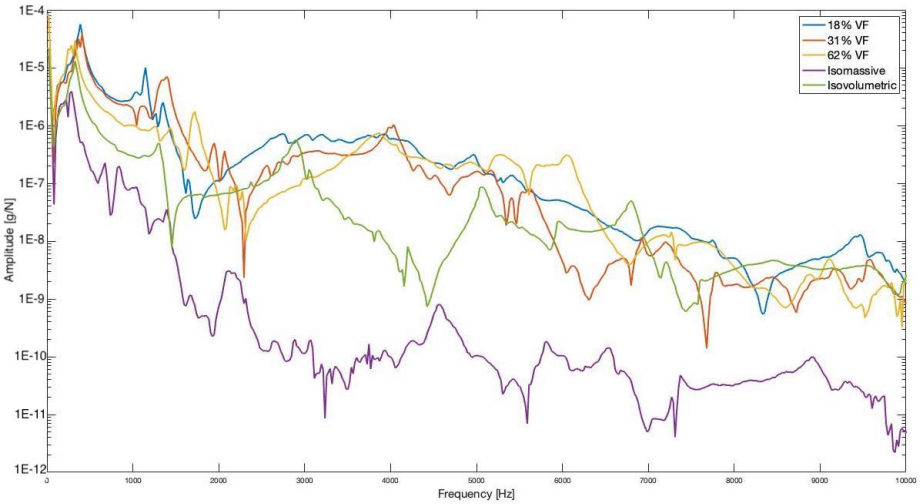

Fig. 5: Acceleration per unit force of various closed-wall specimens alongside control specimens without filling oil.

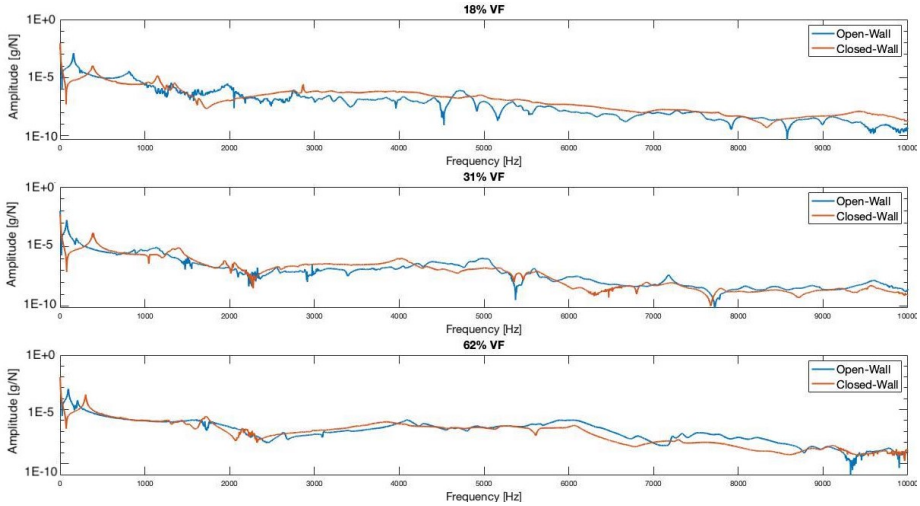

Fig. 6: Acceleration per unit force: comparing open- and closed-wall specimens.

a much larger sandwich structure that would be used in spacecraft structures. The boundary effects and errors due to the 3D printing would have less impact on the global dynamics if a larger size specimen was 3D-printed and tested.

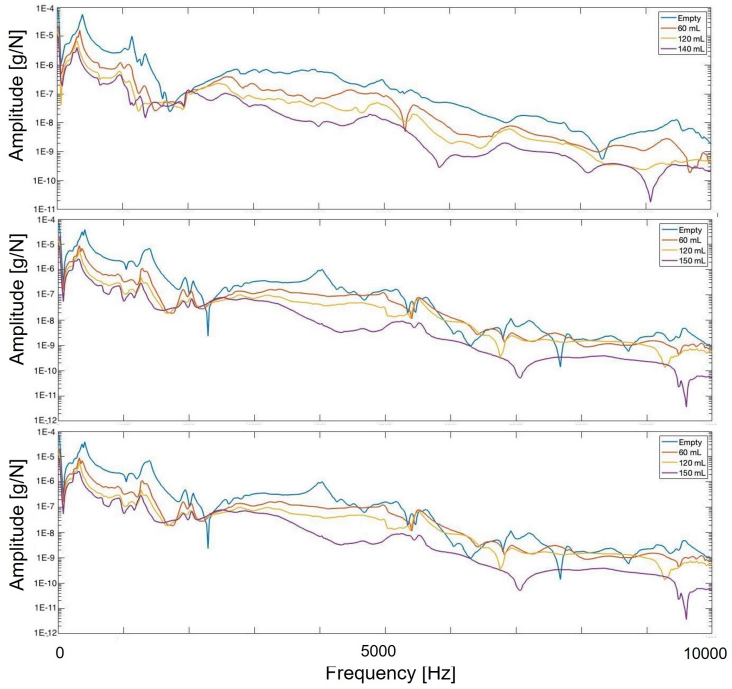

Fig. 7: Acceleration per unit force of various closed-wall specimens with and without filled oil.

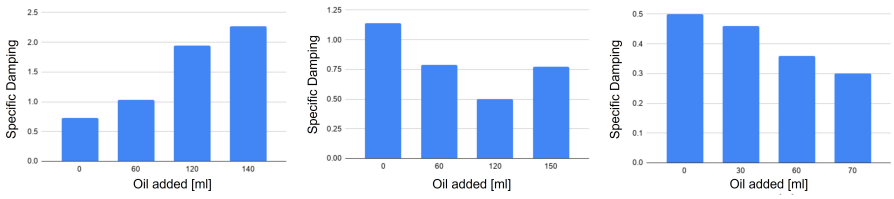

(a) (b) (c)

Fig. 8: Variation of specific damping with added oil for the closed-wall specimens with: a) 18% VF, b) 31% VF, c) 62% VF.

4 Conclusion

This paper investigated the damping properties of FDM 3D-printed, gyroid-based sandwich structures, along with testing the hypothesis that adding a damping element, namely hydraulic oil, that could improve specific damping under volume control. An experimental setup and simulation workflow was designed to facilitate the investigation. The specimens were also compared to the isomassive and isovolumetric specimens for reference. The isomassive specimen

Table 2: Modal Analysis results of sandwich structures.

Mode Number	Isomassive Frequency (Hz)		Isovolumetric Frequency (Hz)		Open-wall 18% VF Frequency (Hz)		Open-wall 18% VF Frequency (Hz)	
	SIMU	EXP	SIMU	EXP	SIMU	EXP	SIMU	EXP
1	481	281	357	330	206	99	1797	389
2	854	1007	524	1338	239	829	2243	1176
3	861	1985	526	2901	429	1925	2254	2792
4	1318	4599	945	5070	1412	3380	2824	3948
5	1319	6268	946	5984	1511	4427	2830	4598
6	1602	7333	1019	6824	1532	4734	3214	5206

with a relatively low mass demonstrates a good damping effect which would be further investigated.

Generally, thicker gyroid-based specimens had lower vibration amplitudes due to their larger mass, as would be expected. Introducing side walls resulted in greater system stiffness for closed-wall specimens, and therefore the first modal peak was reduced and shifted to a larger frequency with a better absorption at the relatively low-frequency range. Further, adding hydraulic oil also reduces vibration amplitude, especially for low volume fraction closed-wall specimens.

There was very little consistency between experimental and simulated specimens in natural frequency analysis. The issues with undissolved support structure material are likely a key contributor, alongside limitations with the simulation workflow, which need to be solved in the next step.

Despite these challenges, the study does warrant future work. AM provides spacecraft engineers with much more design freedom, and incorporating this technology into spacecraft design is certainly a step in the right direction, as shown by its ability to produce promising geometries such as the gyroid. The possible design space of damping structures for space using AM technologies is vast, and the present work only scratches the surface. In future work, different sandwich core geometries will be investigated especially different meta-lattice sandwich structures. For larger specimens, more than one accelerometer should be used. By placing several accelerometers around the specimen (in different orientations), better inferences can be made about mode shapes and modal frequencies, particularly when comparing experimental results to simulations.

References

1. T. Bitzer, Honeycomb technology: materials, design, manufacturing, applications and testing, Springer Science & Business Media, 1997.
2. C. A. Henry, An introduction to the design of the cassini spacecraft, Space science reviews 104 (1) (2002) 129–153.
3. H. Li, Y. Hu, H. Huang, J. Chen, M. Zhao, B. Li, Broadband low-frequency vibration attenuation in 3d printed composite meta-lattice sandwich structures, Composites Part B: Engineering 215 (2021) 108772.

4. G. Palma, H. Mao, L. Burghignoli, P. Göransson, U. Iemma, Acoustic metamaterials in aeronautics, Applied Sciences 8 (6) (2018) 971.
5. A. A. Shapiro, J. Borgonia, Q. Chen, R. Dillon, B. McEnerney, R. Polit-Casillas, L. Soloway, Additive manufacturing for aerospace flight applications, Journal of Spacecraft and Rockets (2016) 952–959.
6. H. Y. Sarvestani, A. Akbarzadeh, A. Mirbolghasemi, K. Hermenean, 3D printed meta-sandwich structures: Failure mechanism, energy absorption and multi-hit capability, Materials & Design 160 (2018) 179–193.
7. H. Mao, R. Rumpler, M. Gaborit, P. Göransson, J. Kennedy, D. O'Connor, D. Trimble, H. Rice, Twist, tilt and stretch: From isometric kelvin cells to anisotropic cellular materials, Materials & Design 193 (2020) 108855.
8. H. Mao, R. Rumpler, P. Göransson, A note on the linear deformations close to the boundaries of a cellular material, Mechanics Research Communications 111 (2021) 103657.
9. H. Mao, M. Gaborit, E. Lundberg, R. Rumpler, B. Yin, P. Göransson, Dynamic behaviour of low-to high-density anisotropic cellular materials, Journal of Sound and Vibration 536 (2022) 117137.
10. A. H. Schoen, Infinite periodic minimal surfaces without self-intersections, Tech. rep. (1970).
11. D. Li, W. Liao, N. Dai, Y. M. Xie, Comparison of mechanical properties and energy absorption of sheet-based and strut-based gyroid cellular structures with graded densities, Materials 12 (13) (2019) 2183.
12. J.-W. Luo, L. Chen, T. Min, F. Shan, Q. Kang, W. Tao, Macroscopic transport properties of gyroid structures based on pore-scale studies: permeability, diffusivity and thermal conductivity, International Journal of Heat and Mass Transfer 146 (2020) 118837.